

## HORIZONTAL STRAIN - SLOPE STABILITY CORRELATION CONSIDERING THE EFFECT OF SHALLOW EXCAVATION NEAR THE SLOPE TOE

Duc Tiep Pham<sup>1</sup>, Nam Hung Tran<sup>1</sup>, Van Hoa Cao<sup>1</sup>, \*Gulnaz Zhairbaeva<sup>2</sup>

<sup>1</sup>Institute of Technique for Special Engineering, Le Quy Don Technical University, Ha Noi, Vietnam;

<sup>2</sup>Department of Civil Engineering, L.N. Gumilyov Eurasian National University, Kazakhstan

\*Corresponding Author, Received: 21 Dec. 2023, Revised: 09 May 2024, Accepted: 25 May 2024

**ABSTRACT:** The stability of a soil slope, as initially estimated by design calculations, may be adversely impacted by construction activities near the slope toe, such as excavating foundation pits. This study aims to evaluate the impact of shallow foundation pit location on existing slope stability. The regression function correlating the factor of safety with average horizontal strain is established to analyze this influence. Numerical simulations of homogeneous slopes using Plaxis 2D software, employing the strength reduction method (SRM), are conducted to determine the horizontal deformation field and factor of safety. From 22 numerical test data, a regression function of the factor of safety and average horizontal strain has been built. The results indicated that only at a distance of less than 2m from the toe of the slope to the excavation edge, the presence of excavation reduces the overall stability of the existing slope. Additionally, for slopes with different heights but similar slope angles and physico-mechanical characteristics, excavations at the same distance from the toe, there is a correlation between the average horizontal strain and the factor of safety. Therefore, establishing the regression function is the basis for giving the level of landslide warning for the existing slopes when one has the measurement of the horizontal strain of the slope.

**Keywords:** Slope, Horizontal strain, Strength reduction method, Factor of safety (FS).

### 1. INTRODUCTION

Landslides are incidents in a geotechnical field that occur due to the displacement of soil layers at the ground surface or underneath. According to a summary of SafeLand [1], Europe is the region with the second highest number of deaths and highest economic losses from landslides compared to other continents in the 20th century, with an estimated 16,000 people dead by landslides. Furthermore, the number of people affected by landslides is much larger than reported. Along with climate change, landslides are also one of the major concerns of Governments in issuing warnings and remedial measures. Landslides are natural disasters that commonly occur in Vietnam [2]. Vietnam's terrain occupies three-quarters of the territory, so the constructions are often adjacent to hills and mountainsides. Thus, the neighboring construction has interfered with the natural slope. It tends to destabilize the slope, such as digging the foot of the slope, but does not have effective measures of reinforcement of the slopes. In addition to the increasing influence of climate change (heavy and prolonged rainfall), the risk of landslides occurring is greater and more serious. Therefore, the detection of landslide risk and early warning about it to minimize damages is necessary and could be an economical solution in the current conditions.

Alongside the development of science and technology, the soil monitoring and data collection

systems utilized in design [3], large-scale experiments have been conducted to assess the strength of the sliding surface during landslide movement to estimate the factor of stability of slope [4]. The rapid development of various monitoring techniques brings new sensing and monitoring techniques, such as fiber optic sensing technology (Fig.1) [5,6,7], micro-electromechanical systems [8], and satellite remote sensing technologies [9] into the area of geological and geotechnical monitoring field. These technologies have greatly improved both the accuracy and scope of monitoring.

To reduce risks due to slope instability, the development of early warning systems based on measured data from the slope has been researched and deployed to establish necessary warning levels [10, 11]. Besides, the rate of change in groundwater levels can impact slope stability [12]. Therefore, remote monitoring systems to detect the surface tilt angles of slopes, ground surface deformation combined with rainfall measurements, water content, and changes in groundwater levels in slopes are also of research interest [13,14,15].

Many previous studies have focused on the determination of the correlation between these measured parameters and the factor of safety, such as the correlations between different soil parameters and the factor of safety of slope, using regression analysis [16]. Besides, the different regression functions are proposed to indicate the dependence of the stability coefficient of the slope on its horizontal

displacements [17,18]. However, the studies have not yet considered the presence of shallow excavation near the toe of the slope, which can affect its stability.

The present paper aims at evaluating the effects of the location of shallow excavation on the stability of the existing slope as well as proposing a regression function showing the correlation between the factor of safety and its average horizontal displacement.

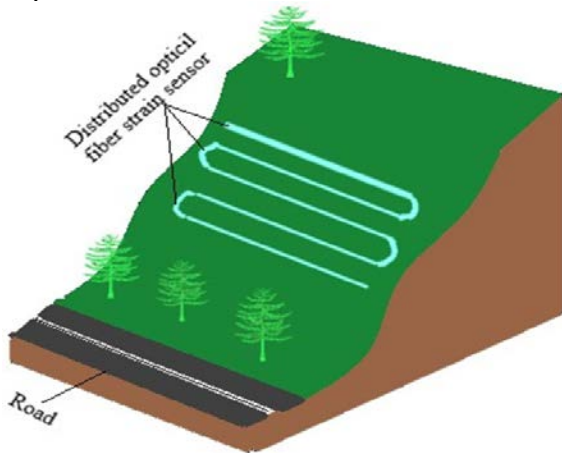


Fig.1 Slope monitoring with fiber optic sensing

In the following part of the article, the authors will present the research significance and evaluations of the sliding stability coefficient of the slopes with and without shallow excavations in the vicinity of the slope toe and in correlation with the horizontal deformation of the slope.

## 2. RESEARCH SIGNIFICANCE

The neighboring construction activities can impact the stability of the slope, particularly due to shallow excavations near the slope toe. This overlooked factor in the design process significantly influences slope stability but has not been adequately addressed in previous studies. This study aims to establish a theoretical foundation for evaluating the stability of existing slopes, taking into account the detrimental effect of shallow excavations at the slope toe, based on data from horizontal strain monitoring. Numerical tests are conducted to assess the impact of the shallow excavation's position on slope stability. The findings of this investigation offer valuable insights into potential risks posed by human activities to existing slopes.

## 3. SLOPE STABILITY COEFFICIENT DETERMINATION UNDER LOAD

To determine the factor of safety, it is possible to use analytical methods, such as Fellenius's classical

method and Bishop's method, or numerical methods such as the finite element method or finite difference method, etc. Numerical methods prove to have many advantages when the slope is composed of many different soil types and/or with complex boundary conditions. In this study, a factor of safety is determined by a numerical approach based on the finite element method.

## 4. SLOPE WITHOUT SHALLOW EXCAVATION IN THE VICINITY OF THE SLOPE TOE

### 4.1 Geometry And Mesure Of Meshing

The geometry model of the problem is illustrated in Fig.2 in which the slope height  $H=10m$  and the slope angle  $\beta=45^\circ$ .

The plan deformation triangular finite elements of 6 nodes are chosen in the geotechnical software Plaxis 2D. The boundary conditions of the problem are as follows. The bottom edge of the model is presented on displacements in both horizontal and vertical directions whilst the left and right lateral edges of the model are presented on horizontal displacements. The surface of the slope is freely deformed.

The soil behavior obeys the Mohr-Coulomb model with the parameters shown in (Table 1).

Table 1 Physico-mechanical characteristics of soil [17]

Unit	Deformation weight	modulus E (kN/m <sup>2</sup> )	Poisson ratio	Adhesive strength, C (kN/m <sup>2</sup> )	Angle of internal friction, $\varphi$ (degree)
20	100 000	0.33	12.50	25	

In the finite element method, the meshing greatly affects the calculated results. With respect to the same slope, different meshing methods, such as coarse meshing or fine meshing, will result in different deformation and stability coefficients. Quadrilateral element mesh is often done in FLAC and ABAQUS software [17,19,20].

In Plaxis 2D software, the finite elements used are triangular elements. The disadvantage of choosing the triangular element is that the obtained results would have a large error if the size of elements is large, in comparison with the quadrilateral elements. Therefore, it is necessary to choose an appropriate meshing method so that the results of the problem most closely reflect the working of the slope. In this study, to obtain the most accurate results, predefined lines are used to generate finite elements (Fig.2). The software Plaxis 2D then divides each quadrilateral into two triangular elements that are compatible with the

finite element defined in the software. This is a measure to overcome the disadvantages of automatic meshing, which generates large triangular elements in the slope body and thereby leads to larger errors in calculation results. Fig.2 and Fig.3 show the quadrilateral grids and finite element grids that were generated on these grid cells, respectively.

In this study, the calculation of the overall sliding stability of the slope is performed by the

strength reduction method SRM (Strength Reduction Method) [17].

In Table 2 and Figs. 4-6, the dependence of the output results (maximum shear strain and sliding stability coefficient) on the finite element meshing measure is clarified.

Table 2 Comparison of calculation results by different types of element meshing

Nº	Meshing measure	Element fineness	Number of triangle elements	Overall coefficient of sliding stability, FS	Maximum shear deformation ( $\mu\epsilon$ )
1	Automatic meshing (Plaxis 2D)	very coarse	48	1.164	90.0
2	Automatic meshing (Plaxis 2D)	coarse	107	1.147	110.4
3	Automatic meshing (Plaxis 2D)	medium	177	1.135	155.9
4	Automatic meshing (Plaxis 2D)	fine	408	1.129	156.70
5	Automatic meshing (Plaxis 2D)	very fine	728	1.110	232.50
6	Meshing on the basis of the preformed quadrilateral grid (Plaxis 2D)		3552	1.068	350.00
7	Quadrilateral meshing (FLAC), [17]		1776 (=3552/2)	1.061	350.00

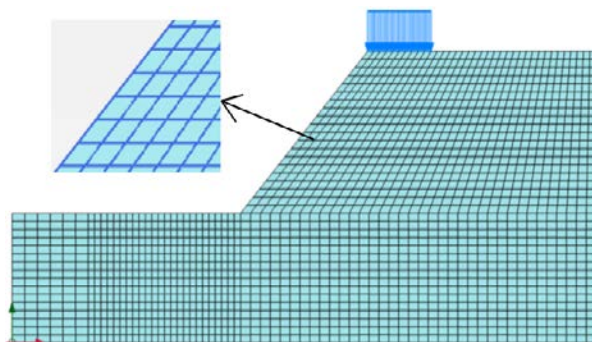


Fig.2 Quadrilateral cells were established

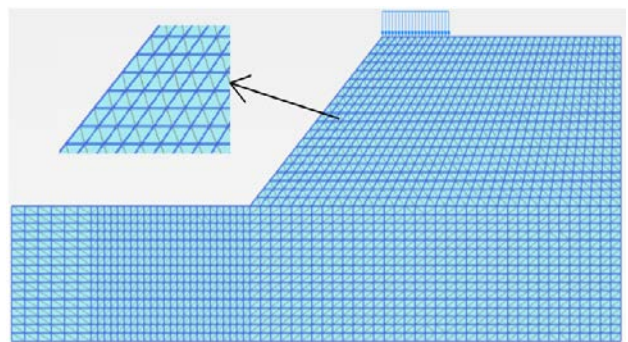


Fig.3 Finite Element Mesh Based on the basis of the original quadrilateral cells

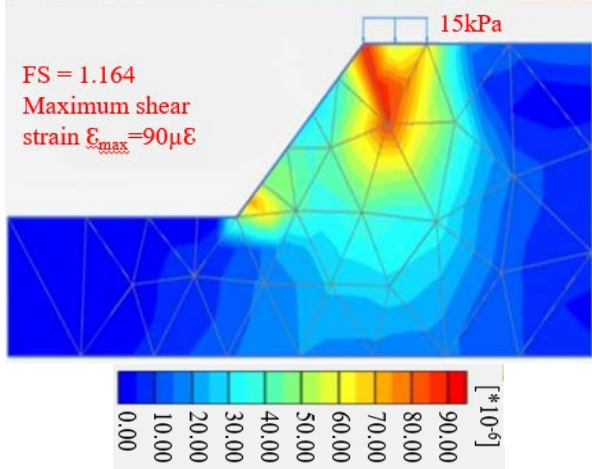


Fig.4 Contours of shear strain with automatic meshing in Plaxis 2D (very coarse)

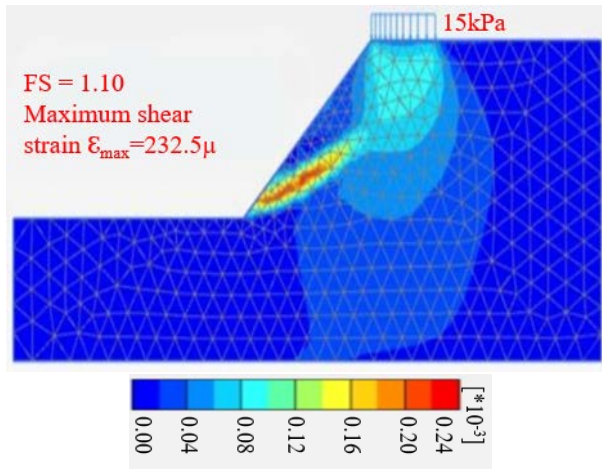


Fig.5 Contours of shear strain with automatic meshing in Plaxis 2D (very fine)

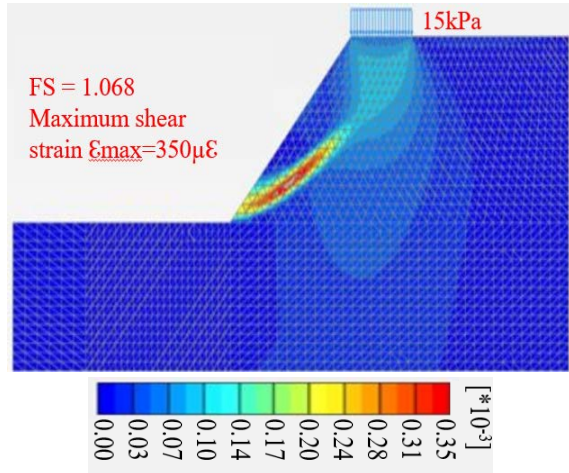


Fig.6 Contours of shear strain with finite element mesh based on the basis of the original quadrilateral cells

From the above results, some comments can be made:

- As predicted, the coarser mesh, the larger the stability coefficient and the smaller the strain;
- The use of automatic meshing and very fine meshing in Plaxis 2D has not yet achieved the desired results. In order to achieve good results, in the case of this problem, the geometry model is divided into the quadrilateral grid and then the meshing is generated based on this quadrilateral grid.

#### 4.2 Changes In Horizontal Deformations And Stability Coefficient

In this part, the change of load intensity from 5 kPa to 35.5 kPa acting on the slope surface with loading range  $b=5\text{m}$  are investigated.

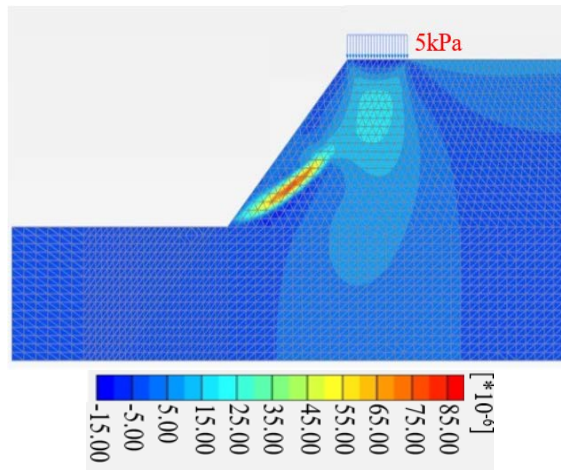


Fig.7 Contours of horizontal strain with surface load  $p=5 \text{ kPa}$  ( $\epsilon_{xx}^{\max}=87.28 \mu\epsilon$ ; FS=1.10)

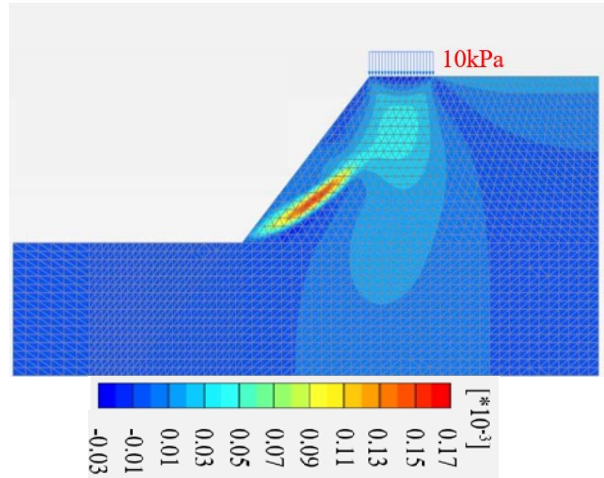


Fig.8 Contours of horizontal strain with surface load  $p=10 \text{ kPa}$  ( $\epsilon_{xx}^{\max}=169.30 \mu\epsilon$ ; FS=1.085)

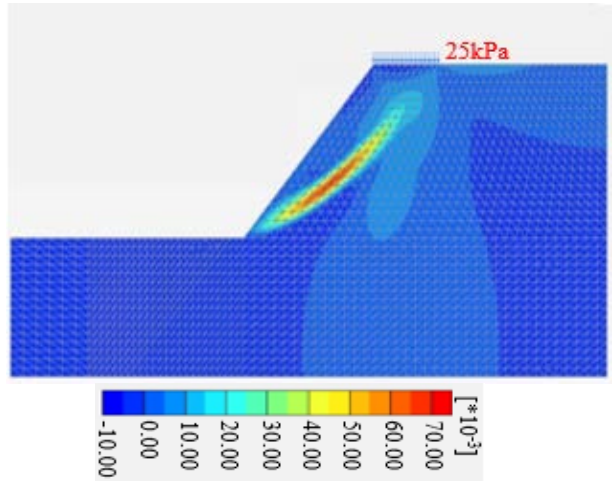


Fig.9 Contours of horizontal strain with surface load  $p=25 \text{ kPa}$  ( $\epsilon_{xx}^{\max}=745.10 \mu\epsilon$ ; FS=1.022)

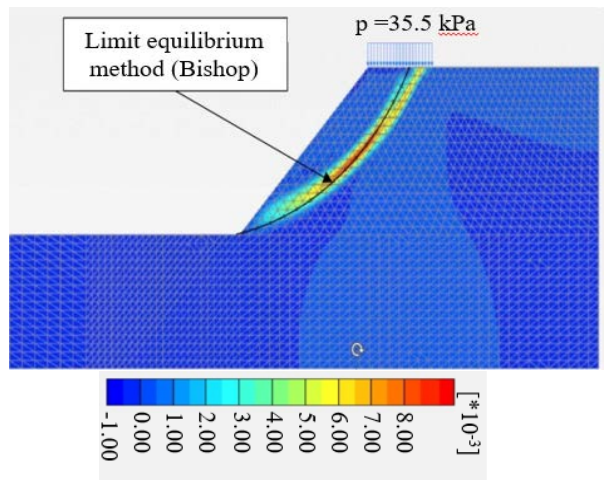


Fig.10 Contours of horizontal strain with surface load  $p=35.5 \text{ kPa}$  ( $\epsilon_{xx}^{\max}=7823 \mu\epsilon$ ; FS=1.006)

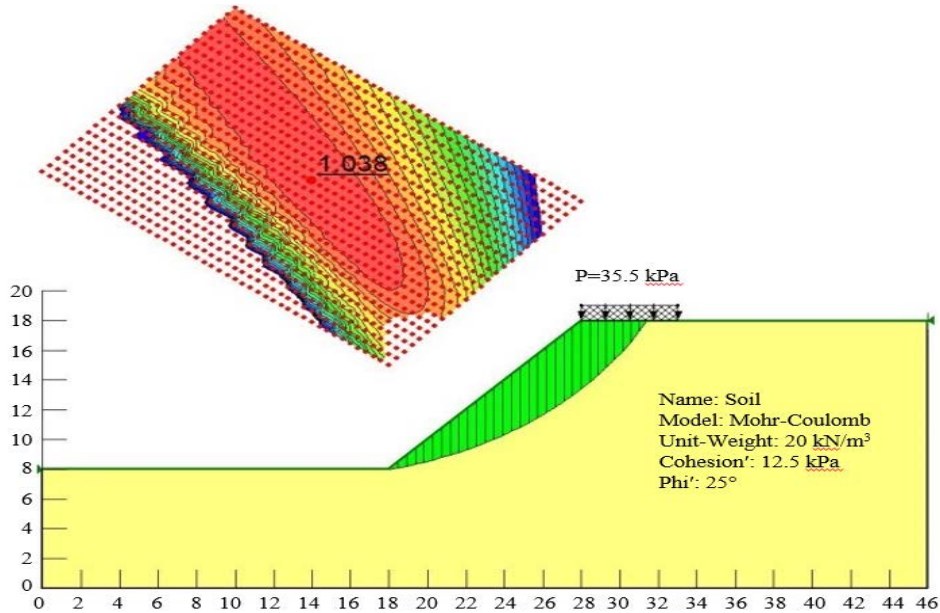


Fig.11 Calculation of slope stability according to Bishop method with surface load  $p=35.5$  kPa

The results show that (see Fig.7 to Fig.11):

- As expected, the higher the load, the greater the lateral deformation and the lower the coefficient of stability;
- Horizontal strain increases suddenly when the slope is in a state of near instability ( $FS \approx 1.00$ );
- If the load is increased, the locus of the maximum horizontal strain points develops upward from the foot of the slope. When the unstable state is nearly reached, the locus of the maximum horizontal strain points forms a sliding arc that develops from the toe to the top of the slope, with the form closed to the sliding arc determined by the Bishop limit equilibrium method.

## 5. SLOPE WITH SHALLOW EXCAVATION IN THE VICINITY OF THE SLOPE TOE

### 5.1 Analysis Of The Influence Of Closely Located Excavation On Slope Stability

In this part, the influence of shallow excavation on the slope stability is investigated. Dimensions of the trapezoidal excavation are chosen as follows (Fig.12): the excavation bottom width  $b=3$ m; the excavation crater width  $B=8$ m; the excavation depth  $h=2.5$ m. The distance from excavation edge to the slope toe changes in range of  $L=0 \div 3.0$ m [21]. With regard to the slope, two heights of slope are taken into account,  $H=8$ m and  $H=10$ m.

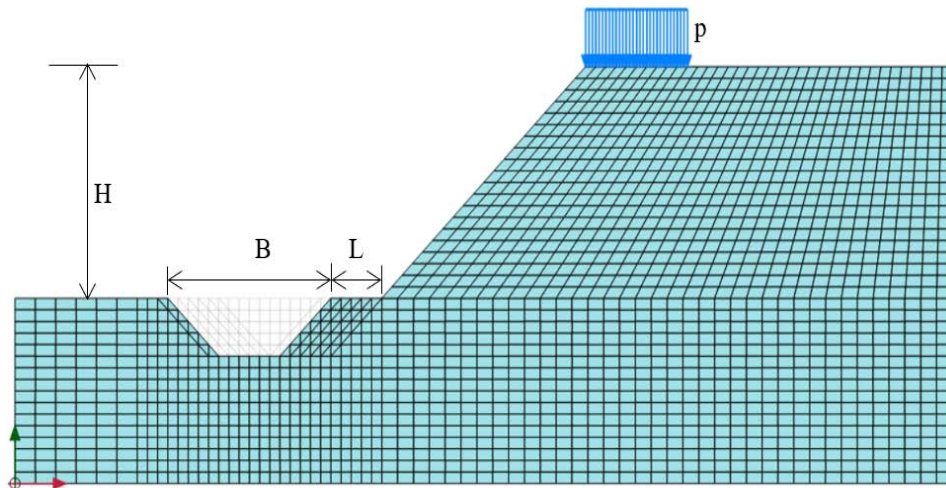


Fig12 Slope with the shallow excavation in the vicinity

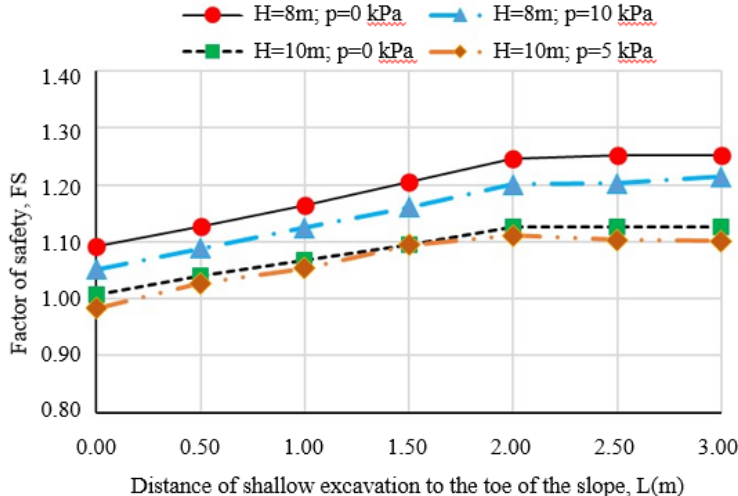


Fig.13 Correlation factor of safety and the position of the shallow excavation

Fig.13 shows the correlation between the factor of safety and the location of excavation. It can be observed that, at a distance inferior to 2m from the slope toe, the excavation reduces the overall coefficient of sliding stability of the slope.

## 5.2 Regression Relationship Between Deformation And Safety In Shallow Excavation

The correlation between the factor of safety and the average lateral deformation of the slope, regardless of the shallow excavation at the slope toe, is shown below [17].

$$FS = a \cdot \varepsilon_{tb}^{-b} + c \quad (1)$$

where  $a$ ,  $b$ , and  $c$  are constants, and  $\varepsilon_{tb}$  is the mean horizontal deformation of the slope.

As presented above, with a distance less than 2m from the excavation edge to the slope toe, FS

value is influenced by the presence of the excavation. Therefore, in order to evaluate effect of the shallow excavation on the slope stability, the distance from the excavation edge to the slope toe  $L=1m$  is choosed. Three heights of the slope,  $H=6m$ ,  $H=8m$  and  $H=10m$ , are taken in account. The other parameters of the slope and the soil are chosen as previous parts. On the slope surface, the load is distributed in the width range of  $b=H/2$ ; the load value increases until the factor of safety is approximately 1.00.

Table 3 shows a database set with 22 different problems built to establish the correlation between the average horizontal strain and FS value.

On the basis of the database in Table 3, the regression function has the form of formula (1) and uses the Solver tool in MS Excel. The regression equation is determined as follows:

$$FS = 3.213576633 \cdot \varepsilon_{tb}^{-0.881342384} + 0.989939089 \quad (2)$$

$R^2 = 0.929$

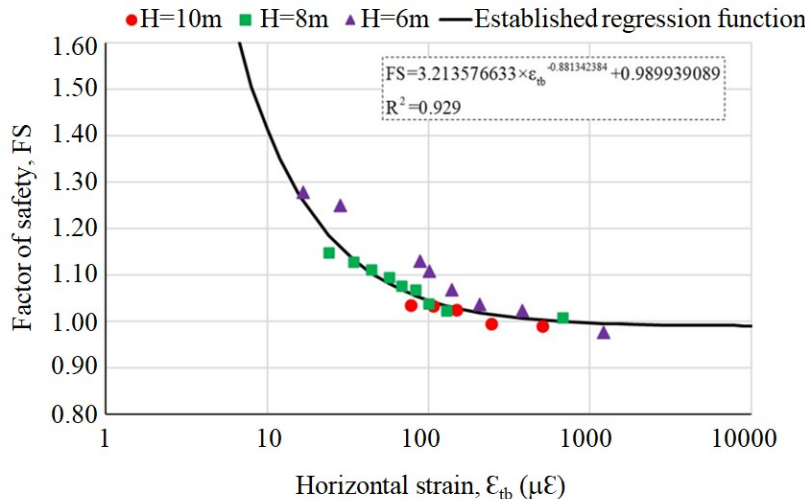


Fig.14 Correlation between stability coefficient and horizontal strain of slope

Table 3 The database were built to establish the correlation between the average horizontal strain and FS value

	Geometric features		Surface Load			Soil characteristics			Average horizontal strain $\epsilon_{tb}$ ( $\mu\epsilon$ )	FS
	H m	$\beta$ degree	b m	p kN/m <sup>2</sup>	$\gamma$ kN/m <sup>3</sup>	E MN/m <sup>2</sup>	$\varphi$ degree	C kN/m <sup>2</sup>		
1	10	45	5	5	20	100	25	12.5	77.50	1.036
2	10	45	5	10	20	100	25	12.5	107.43	1.034
3	10	45	5	15	20	100	25	12.5	148.97	1.026
4	10	45	5	20	20	100	25	12.5	245.90	0.996
5	10	45	5	25	20	100	25	12.5	510.03	0.991
6	8	45	4	5	20	100	25	12.5	24.08	1.148
7	8	45	4	10	20	100	25	12.5	34.16	1.129
8	8	45	4	15	20	100	25	12.5	44.37	1.112
9	8	45	4	20	20	100	25	12.5	56.93	1.095
10	8	45	4	25	20	100	25	12.5	67.65	1.076
11	8	45	4	30	20	100	25	12.5	83.24	1.068
12	8	45	4	35	20	100	25	12.5	100.01	1.039
13	8	45	4	40	20	100	25	12.5	129.43	1.024
14	8	45	4	45	20	100	25	12.5	675.38	1.008
15	6	45	3	5	20	100	25	12.5	16.66	1.279
16	6	45	3	10	20	100	25	12.5	28.50	1.250
17	6	45	3	35	20	100	25	12.5	88.95	1.130
18	6	45	3	40	20	100	25	12.5	101.10	1.109
19	6	45	3	50	20	100	25	12.5	140.00	1.069
20	6	45	3	60	20	100	25	12.5	206.96	1.037
21	6	45	3	70	20	100	25	12.5	380.56	1.024
22	6	45	3	80	20	100	25	12.5	1219.74	0.977

Fig.14 shows that there is a clear correlation between the average horizontal strain and the stability coefficient. Based on the data of 22 numerical tests, a regression function of slope safety coefficient and average horizontal strain has been built with an accuracy of  $R^2=0.929$ . With respect to the regression function established, the following comments can be made:

- The smaller the average horizontal strain, the higher the stability coefficient and vice versa;
- When the horizontal strain is large, the regression function graph is asymptotic to the line  $FS=0.989939089$ ;
- This regression function is the basis for giving the level of landslide warning for the existing slopes when one measures the horizontal strain of the slope.

## 6. CONCLUSION

Based on numerical simulations of the homogeneous slope using Plaxis 2D software to determine the horizontal deformation field and the overall sliding coefficient according to the intensity reduction method (SRM), some conclusions are given as follows:

- The deformation field and FS value depend on the meshing measure, and thus, it is necessary to choose an appropriate meshing. In this study, the software Plaxis 2D are used to generate mesh based on the preformed quadrilateral grid in the geometric model of the problem;

- If the load on the slope surface is increased, the locus of the maximum horizontal strain points develops upward from the toe of the slope. When nearly reaching the unstable state, the locus of the maximum horizontal strain points forms a sliding arc that develops from the toe to the top of the slope;

- The excavation of foundation pits near the toe of the existing slope would increase the risk of landslides. Within the scope of this study, the results of numerical simulations showed that only at a distance of less than 2m from the toe of the slope to the excavation edge, the presence of excavation reduces the overall coefficient of sliding stability of the existing slope;

- If the slopes have different heights but the same slope angle and physico-mechanical properties and have excavations at the same distance from the toe of the slope, there is still a correlation between the average horizontal strain and the stability coefficient. The regression function is the basis for giving the level of landslide warning for the existing

slopes when one has the measurement of the horizontal strain of the slope.

## 7. REFERENCES

- [1] Lacasse, S., and Nadim, F. Landslide risk assessment and mitigation strategy. *Landslides–disaster risk reduction*, 2009, pp.31-61.
- [2] Nguyen, C.T., Ha, K.T., and Vo, T.N. Landslide warning system. Collection of scientific reports for the period 2011-2015, Duy Tan University (in Vietnamese).
- [3] Zhussupbekov A., Sarsembayeva A., Experimental study of deicing chemical redistribution and moisture mass transfer in highway subsoils during the unidirectional freezing. *Transportation Geotechnics*, Vol. 26, 2021.
- [4] Ishii, Y., Ota, K., Kuraoka, S., and Tsunaki, R. Evaluation of slope stability by finite element method using observed displacement of landslide. *Landslides*, Vol. 9, 2012, pp. 335-348.
- [5] Culshaw, B., and Kersey, A. Fiber-optic sensing: A historical perspective. *Journal of lightwave technology*, 2008, 26(9)pp.1064-1078.
- [6] Li, F., Zhao, W., Xu, H., Wang, S., & Du, Y. A highly integrated BOTDA/XFG sensor on a single fiber for simultaneous multi-parameter monitoring of slopes. *Sensors*, Vol. 19(9), 2019, pp. 2132.
- [7] Ye, X., Zhu, H. H., Wang, J., Zhang, Q., Shi, B., Schenato, L., and Pasuto, A. Subsurface Multi-Physical Monitoring of a Reservoir Landslide With the Fiber-Optic Nerve System. *Geophysical Research Letters*, 49(11)-2022 e2022GL098211.
- [8] Towhata I., Uchimura T., Seko I., and Wang L., Monitoring of unstable slopes by MEMS tilting sensors and its application to early warning. In IOP conference series: earth and environmental science Vol. 26, No. 1, 2015, p. 012049.
- [9] Wang, J., Xiang, W., and Lu, N. Landsliding triggered by reservoir operation: a general conceptual model with a case study at Three Gorges Reservoir. *Acta Geotechnica*, 2014, 9, pp.771-788.
- [10] Intrieri, E., Gigli, G., Mugnai, F., Fanti, R., and Casagli, N. Design and implementation of a landslide early warning system. *Engineering Geology*, (2012). 147, pp.124-136.
- [11] Ju N.P., Huang J., Huang R.Q., He C.Y., and Li Y.R.A Real-time monitoring and early warning system for landslides in Southwest China. *Journal of mountain science*, Vol. 12 - 2015, pp. 1219-1228
- [12]. Utепов, Y., Zhussupbekov, A., Aldungarova, A., Mkilima, T. The influence of material characteristics on dam stability under rapid drawdown conditions. *Archives of Civil Engineering*, Vol. 68(1), 2022, pp. 539–553
- [13] Lin W., Shunsaku N., Taro U., Ikuo T., Ling S., and Shangning T., An early warning system of unstable slopes by multi-point MEMS tilting sensors and water contents. In *Advancing Culture of Living with Land*.
- [14] Sheikh, M. R., Nakata, Y., Shitano, M., and Kaneko, M. Rainfall-induced unstable slope monitoring and early warning through tilt sensors. *Soils and Foundations*, 2021, 61(4), pp.1033-1053.
- [15] Sheikh, M. R., Nakata, Y., Shitano, M., and Kaneko, M. Rainfall-induced unstable slope monitoring and early warning through tilt sensors. *Soils and Foundations*, 2021, 61(4), pp.1033-1053.
- [16] Sheikh, M. R., Nakata, Y., Shitano, M., and Kaneko, M. Rainfall-induced unstable slope monitoring and early warning through tilt sensors. *Soils and Foundations*, 2021, 61(4), pp.1033-1053.
- [17] Sheikh, M. R., Nakata, Y., Shitano, M., and Kaneko, M. Rainfall-induced unstable slope monitoring and early warning through tilt sensors. *Soils and Foundations*, 2021, 61(4), pp.1033-1053.
- [18] Khan, M. I., and Wang, S. Slope Stability Analysis to Develop Correlations between Different Soil Parameters and Factor of Safety Using Regression Analysis. *Polish Journal of Environmental Studies*, 2021. 30(5).
- [19] Wang, Z., Zhang, W., Gao, X., Liu, H., and Böhlke, T. Stability analysis of soil slopes based on strain information. *Acta Geotechnica*, 2020. 15, pp. 3121-3134.
- [20] Zhu, H. H., Shi, B., Yan, J. F., Chen, C., Li, Y., Wang, J., and Zhang, J. Physical model testing of slope stability based on distributed fiber-optic strain sensing technology. *Chinese Journal of Rock Mechanics and Engineering*, Vol. 32 № 4, 2013, pp.821.
- [21] Kim, J., Jeong, S., and Regueiro, R. A. Instability of partially saturated soil slopes due to alteration of rainfall pattern. *Engineering Geology*, Vol. 147 2012,pp. 28-36.
- [22] Shaldykova, A., Moon, Sung -Woo, Kim, J., Lee, D., Ku, T., Zhussupbekov, A., Comparative analysis of Kazakhstani and European approaches for the design of shallow foundations. *Applied Sciences (Switzerland)* Vol. 10, Issue 81, 2020.
- [23] Duong, H. H., Nguyen, X. Tr. Highway design, Vol. 2, Education Publisher, 2004 (in Vietnamese).